

## INTERACTIONS OF THE MESOPOROUS SILICA-CAPTOPRIL NANOCOMPOSITES WITH SOME METABOLIC PROCESSES IN MONKEY KIDNEY *VERO CELLS*

R. F. POPOVICI<sup>a</sup>, C.T. MIHAI<sup>b</sup>, E.M.SEFTEL<sup>c</sup>, P. ROTINBERG<sup>b</sup>,  
E. POPOVICI<sup>\*</sup>, V. A.VOICU<sup>a</sup>

<sup>a</sup>*University of Medicine and Pharmacy "Carol Davila", Department of Clinical Pharmacology and Toxicology, Bucharest, Romania*

<sup>b</sup>*Department of Cell Biology, Biological Research Institute, Iasi, Romania*

<sup>c</sup>*Department of Materials Chemistry, Faculty of Chemistry, "Al. I.Cuza" University, Iasi, Romania*

(Received March 21, 2011; Accepted June 8, 2011)

*Keywords:* Mesoporous silica, Captopril, Nanocomposites, Monkey kidney *Vero cells*, Metabolic processes

### 1. Introduction

One of the contemporary scientific research priorities is related to the potentiation of the currently available formulations of drug molecules in the direction of improvement of their effectiveness, at the same time maintaining an acceptable safety profile.

The progress done in this direction has created one of the most dynamic science and technology domains at the confluence of physical sciences, molecular engineering, biology, biotechnology and medicine [1-3]. The field of nanotechnology has motivated researchers to develop nanostructured materials for biomedical applications, in order to create controlled released drug delivery systems that promise to solve the challenge of poor biodisponibility of drugs and to maintain the desired release rate throughout the dosage period, in order to safely increase their effectiveness [4-6].

One of the solutions considered is the optimization of the effect of drug molecule through the use of rationally designed drug carrier materials. The concept of drug delivery systems has emerged to broaden the use of the drugs, expand the ways of their administration minimize their toxic side effects and to solve absorption problems [7].

The characteristics required for a material to be defined as a drug delivery system are as follows: biocompatibility, low toxicity, ability to absorb high loading of drug molecules, lack of susceptibility to premature release, tissue specificity and site orientation, controlled release with a proper rate for an effective local concentration [8]. In this context, the ordered mesoporous silica raises a particular interest in nanomedicine because they meet these conditions [9].

For a couple of years, investigations were performed for evaluating the role of mesoporous silicates in drug and antigen delivery [7,10], tissue engineering [11], gene transfection and cell tracking [7,8,12,13]. As matrix for controlled delivery systems mesoporous silica proved important features: an ordered pore network, homogeneity in size, which allows fine control of the drug load and release kinetics; a generous pore volume (up to 1.2 cm<sup>3</sup>/g) to host the required amount of drugs; a high surface area (up to 1500 m<sup>2</sup>/g), which implies high potential for drug adsorption; a silanol-containing surface that allows functionalization for a better control over drug loading and release [2-5,9].

Recent investigations looked into the biocompatibility and cytotoxicity of mesoporous silica nanomaterials [14-18] and concluded that these materials influence the cell biology by weakening the cell membrane integrity, diminishing cell metabolism and increasing apoptotic

---

\*Corresponding author: eveline@uaic.ro; evelinepopovici@yahoo.com,

signaling. Other research fails to identify a significant cell death of cell culture when treated with the aminated mesoporous silica nanoparticles (MSNs) [19].

This research focused on the evaluation of a modified formulation of cardiovascular drug to assess toxicity and impact on metabolic parameters. The selected cardiovascular therapeutical medication class was the one of inhibitors of angiotensin converting enzyme (ACE). ACEs are one of the most important group of drugs that are used for controlling blood pressure, treating heart failure, preventing strokes, and preventing kidney damage in people with hypertension or diabetes. Out of ACEs, captopril was chosen in this research as loaded drug on MSN, because it is the best documented ACE inhibitor in terms of clinical and metabolic effect. It inhibits the active sites of the zinc glycoprotein ACE, blocking the conversion of angiotensin I to angiotensin II, the latest triggering the entire cascade of reactions responsible for the clinical symptoms and histological modifications in patients with hypertension [20]. Captopril may be used to treat hypertension, congestive heart failure and renal nephropathy.

The dimensions of captopril molecule (Figure 1a) are 0.9 x 0.57 x 0.33 nm and it includes a thiol group, an amide group, an acid carboxylic group and a chiral carbon atom (Figure 1b). Captopril is a zwitterionic drug, with two dissociation constants,  $pK_{a1}$  3.7 and  $pK_{a2}$  9.8, and has an isoelectric point of 6.8. In clinical practice, captopril is mainly administrated orally, however injectable preparations are available and used in special cases [21].

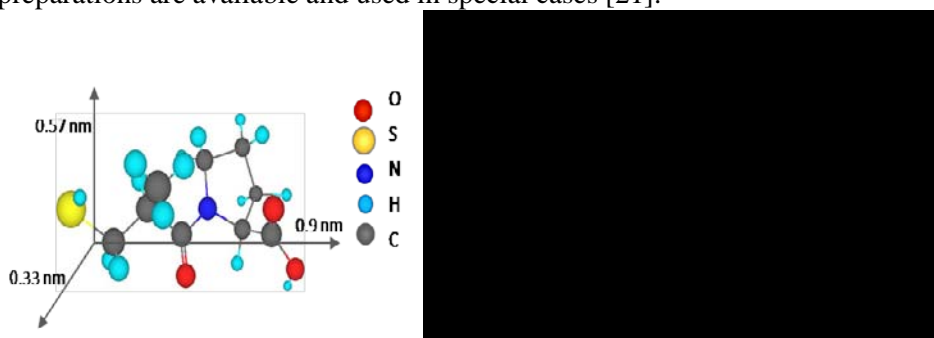


Fig. 1. a) Schematic geometrical representation of captopril molecule; b) Chemical formula of captopril (2S)-1-[(2S)-2-methyl-3-sulfonylpropanoyl]pyrrolidine-2-carboxylic acid.

Knowing the pharmacodynamic properties of captopril and the mesoporous silicates qualities as a drug delivery matrix and vehiculating system, we considered opportune to investigate the impact of captopril loaded onto a mesoporous silica carrier as a potential new formulation for captopril and also to assess the impact on metabolic cell activity.

In a previous paper the influence of processing parameters of ordered mesoporous matrices for the loading and release of captopril was investigated. The release of captopril was controlled by tailoring the surface properties of the mesoporous silica via functionalization. The loading and release kinetics (*in vitro* in simulated gastric and intestinal fluids) showed that both of them were affected by the surface properties of the mesoporous silica materials [22].

In this study we investigated the *in vitro* toxicity of various captopril formulations and their impact on the metabolism of healthy monkey kidney *Vero cells* cultures.

Herein, we described the captopril action, used either as free form or loaded on siliceous matrices: the mesoporous silica matrix type SBA-15 (matrix 1) and functionalized mesoporous matrix SBA-15\_APTES (matrix 2). The modulation of the metabolism of healthy cells was analysed on the basis of biochemical indices (insoluble, soluble and total proteins; glycogen, glucose and lactic acid; total lipids and free fatty acids; DNA, RNA and total nucleic acids).

## 2. Experimental

In the current study the following materials were analysed: SBA-15 (matrix 1), SBA-15 loaded with captopril at room temperature (captopril delivery system 1) and APTES functionalised SBA-15 (matrix 2) loaded with captopril at room temperature (captopril delivery system 2).

## 2.1. Materials preparation

Mesoporous silica SBA-15 (matrix 1) was synthesized by self-assembly from a silica-surfactant liquid-crystal phase, using the modified hydrothermal method reported by Zhao et al. [23]. The molar composition of the mixture was: TEOS:5.87HCl:194H<sub>2</sub>O:0.017P123. First, the initial mixture was subjected to ultrasonic irradiation for 30 minutes in an open glass container (Sonics Materials VCX600, 20 kHz, 13 nm Ti horn). After the ultrasonic step, the solution temperature was measured to be 60°C. The resulting mixture was subjected to hydrothermal process realized at 80°C. The as-synthesized matrix was dried at room temperature and calcined under air flow at a heating rate of 1 C°/min up to 550°C, for 6 h.

In this preparation experiment, as illustrated in Figure 2, the following chemicals were used: tetraethylorthosilicate (TEOS 98%, Acros Organics) as silica source, HCl, triblock copolymer Pluronic P123 (EO<sub>20</sub>PO<sub>70</sub>EO<sub>20</sub>, Aldrich) as polymeric template. The matrix 2 preparation was realized by the surface modification of matrix 1, via silylation method [24], with 3-aminopropyl-triethoxysilane (APTES, Aldrich), as surface functionalizing reagent. Captopril powder was purchased from the Company Sigma-Aldrich (catalog product number C4042).

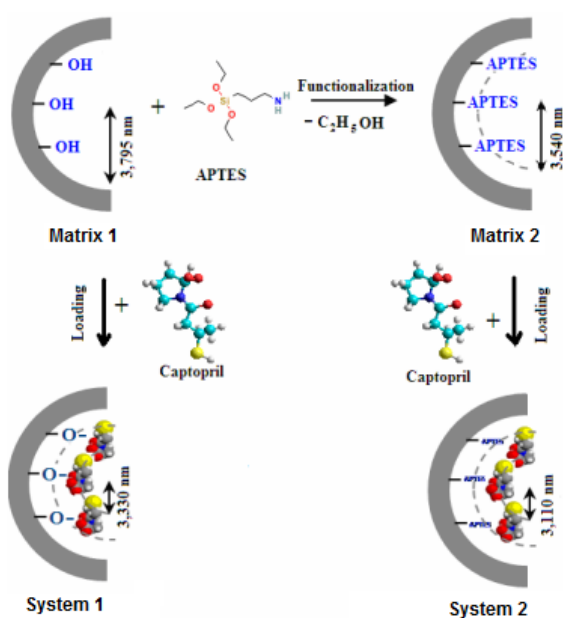


Figure 2. Schematic representation of samples preparation.

The captopril incorporation on both matrices was carried out by wetness impregnation method using a ratio matrix/captopril solution of 220mg/10mL (0.1M) and soaked for 3 days under continuous stirring, at room temperature. The solids were recovered by filtration at the same temperature and dried under vacuum in a desiccator. The obtained samples were denoted as system 1 and system 2, respectively.

## 2.2. Biological material

The biological material used for the *in vitro* experiments was represented by mycoplasma-negative, stabilized, normal *Vero cells*, obtained from *Cercopithecus Aethiops* monkey kidneys and cultured in DMEM growing medium (Dulbecco's Modified Eagle's Medium, Biochrom AG, Germany, FG 0415), supplemented with 10.0% fetal bovine serum (Sigma, Germany, F9665), 100 µg/mL streptomycin (Biochrom AG, Germany, A 331- 26), 100 IU/mL penicillin (Biochrom AG, Germany, A 321-44) and 50 µg/mL antimycotic amphotericin B (Biochrom AG, Germany, A

2612), at a density of  $2 \times 10^6$  cells / 300 cm<sup>2</sup> flask, in a humidified 5% CO<sub>2</sub> atmosphere at 37°C [26]. The reason for selecting this type of cells for the *in vitro* experiment was mainly related to the involvement of renal cells in the control of hypertension and main place of action of ACE inhibitors and its use previously reported in the literature in *in vitro* captopril evaluations [27-29].

The cells were incubated for a period of 144 hours, with growing medium renewed twice. When the cells reached confluence in the monolayer stage, the cultures were divided into control (*Vero cell* culture with no added substance, group A) and 4 groups of cell cultures treated with studied materials: free captopril, (group B – 100% captopril), matrix 1 (group C – 0% captopril), system 1 (group D – 22.59 % captopril) and system 2 (group E- 26.01% captopril), each of them in a dose of 0.4 µg/flask.

The control and treated cultures were incubated another 12 hours, under the same conditions. After this long time treatment, the medium was discarded from the test flasks, the layers of cells were washed with PBS (Saline Phosphate Buffer, Biochrom AG, Germany, L 1825) and then detached from the flasks with 0.25% trypsin + 0.02% EDTA (ethylenediaminetetraacetic acid, Biochrom AG, Germany, L 2163). The cells were pelleted in cylindrical glass tubes by centrifugation at 1.800 rpm for 2 minutes and were weighted for setting the cellular mass/flask representing different experimental groups.

### 2.3. Characterization methods

The structure of both the mesoporous matrices and the prepared systems was characterized by a combination of physical techniques.

X-ray diffraction analysis (XRD) was employed to identify and characterize the morphology of the synthesized materials. The XRD patterns were recorded using a TUR M-62 powder diffractometer system with CuK $\alpha$  radiation ( $K_{\alpha} = 0.1518 \text{ \AA}$ , 36 kV, 20 mA), a voltage of 36 kV, a current of 20 mA, and a goniometer speed of 0.5°/min). The  $a_0$  parameter, calculated by relation  $a_0 = 2d_{100} / \sqrt{3}$ , where  $d$  is interplanar spacing, was used for defining wall thickness ( $t$ ) in the following relation:  $t = a_0 - \text{BJH pore diameter}$ .

BET (Brunauer, Emmett and Teller) specific surface areas ( $S_{\text{BET}}$  (m<sup>2</sup>/g) were obtained from the nitrogen adsorption experiments measured at -196°C after degassing the samples below 10<sup>-3</sup> Torr at 473 K for 2 h on NOVA 2200e (Quantachrome Instruments, Boynton Beach, FL, USA). The pore size distribution was determined from the desorption branch of the isotherm using BJH (Barrett-Joyner-Halenda) method. The total pore volume (TPV, cm<sup>3</sup>/g) was calculated as the amount of nitrogen adsorbed at the relative pressure of cca 0.99.

Particles size distribution and mean pore diameter ( $D_p$ , nm) measurements were recorded using an optic measurement device SALD-7001 type Laser Diffraction Particle Size Analyzer (Shimadzu, Japan). The SEM images were obtained using a Quanta™ Scanning Electron Microscope, operating at an accelerating voltage of 30 kV.

The amount of captopril loaded was monitored by UV–Vis spectrophotometry at 285 nm [25].

### 2.4. Investigational biological methods

The cell pellets of control and treated cultures were resuspended in an adequate volume of 0.88 M sucrose – 0.2 M Tris – HCl buffer, homogenised by ultrasonication on ice with Bandelin – Germany Sonopuls device (2 minutes, 80 cycles/sec/75% power) and centrifuged for 15 minutes at 5.500 rpm, in a swing-out rotor, for obtaining the cell clarified lysates. All operations were performed at 4°C. Adequate aliquots were used for the biochemical determination of some metabolic indices: glycogen (G), glucose (g) and lactic acid (L.A.); total lipids (T.L.), free fatty acids (F.F.A); soluble (S.P.), insoluble (U.P) and total proteins (T.P.); deoxyribonucleic acid (DNA), ribonucleic acid (RNA) and total nucleic acids (TNA) [30].

Glycogen content of *Vero cell* cultures was determined by the anthrone-reagent method [31]. The amount of glucose in the cell cultures was estimated using the *ortho*-toluidine spectrophotometric method [32]. For lactate determination and quantification was used the method described by Barker and Summerson, while for the free fatty acids the method used was with

diphenylcarbazide [33]. The content of total lipids determination was realized by the method E. Chabrol and R. Charonnat based on sulfo-phospho-vanillic reaction [34]. Protein content was quantified by Lowry method [35]

The extraction and purification of DNA and RNA was realized with the automated extractor Maxwell<sup>®</sup> 16 from Promega. For the extraction of the DNA was used the Maxwell<sup>®</sup> 16 DNA Purification Kit (Promega, TM284) and for the RNA extraction was used the Maxwell<sup>®</sup> 16 Total RNA Purification Kit (Promega, TB351). The quantification of the total DNA and RNA, extracted and purified with Maxwell<sup>®</sup> 16 automated extractor, were estimated by spectrophotometry, at wave length of 260 nm, 1 unit of absorbance at 260 nm being equal with 50 µg /mL of DNA or 40 µg /mL of single-stranded RNA.

## 2.5. Statistical analysis

Five tubes of cultures have been used for each culture type, the results being analyzed statistically by means of equal variance Student „t” test [35]. The statistical analysis of the data was realized with Data Analysis package in MS Excel, the level of significance in all statistical analyses was set at a probability of minimum  $p < 0.05$ .

## 3. Results

### 3.1. Nanocomposites characterization

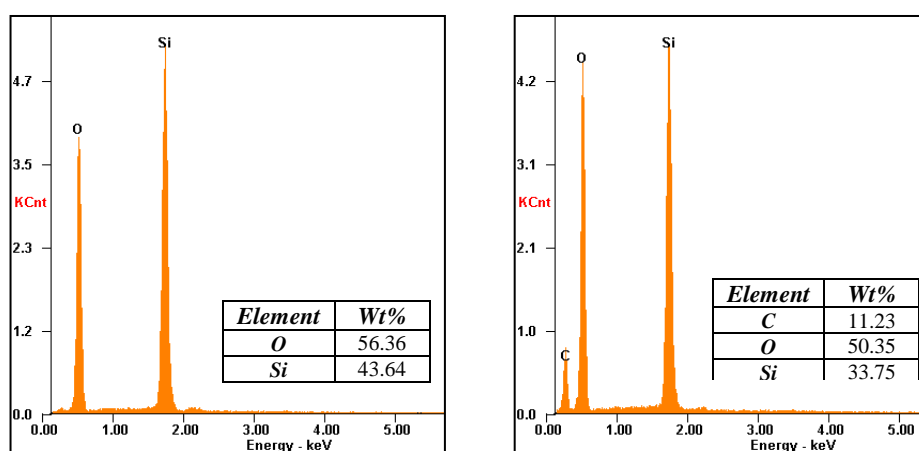
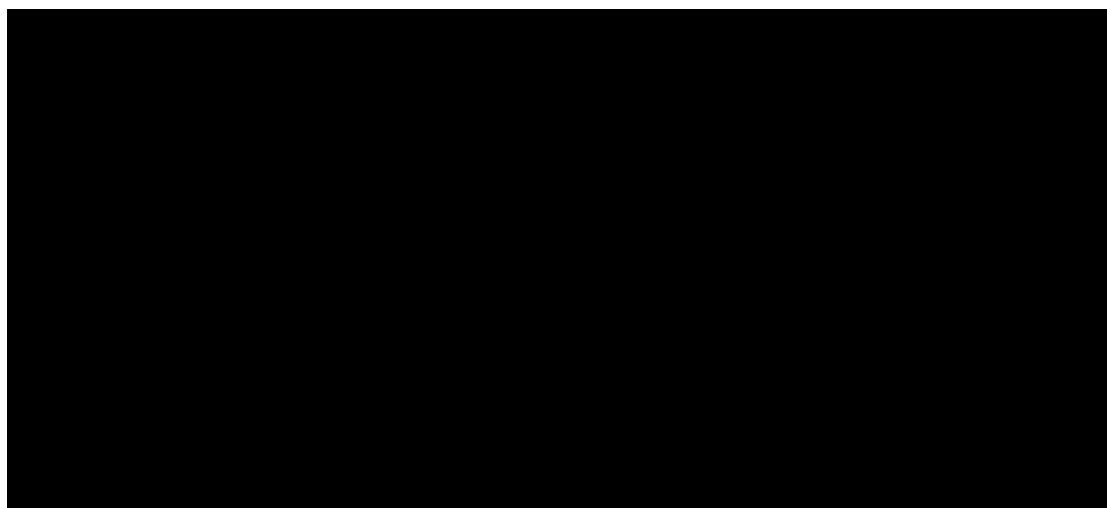


Fig. 3. SEM images of the system 1 (A) and system 2 (B) and EDAX comparative results for matrix 1 and system 1, respectively.

The prepared matrices have a stable mesoporous structure, ordered pore network, high surface area (as shown in Table 1.), and particle size of 480nm and 508nm, respectively (not presented here).

*Table 1. Textural properties of the studied materials.*

Sample	$a_0$ (nm)	$S_{\text{BET}}$ ( $\text{m}^2/\text{g}$ )	TPV ( $\text{cm}^3/\text{g}$ )	$D_p$ (nm)	$t$ (nm)	microS ( $\text{m}^2/\text{g}$ )	microV ( $\text{cm}^3/\text{g}$ )
Matrix 1	9.61	862	0.927	7.59	2.025	375	0.182
Matrix 2	9.61	275	0.431	7.08	2.535	51	0.023
System 1	10.72	509	0.832	6.67	4.12	19	0.045
System 2	10.20	261	0.474	6.22	3.98	4	0.014

Compared with the calcined matrix (550°C for 6 h (1°C/min)), the BET surface area ( $\text{m}^2/\text{g}$ ), diameter pore size ( $D_p$ , nm), and total pore volume (TPV,  $\text{cm}^3/\text{g}$ ) were reduced after the captopril has been loaded, confirming that the captopril was loaded inside the matrix mesopores. An apparently observed increase of pore wall thickness (calculated by  $a_0 - \text{BJH}$  pore diameter) stresses also the captopril entrapment inside the matrix mesopores.

The captopril-loaded SBA-15 matrices (system 1 and 2) showed a decrease both in the micropore surface area (microS,  $\text{m}^2/\text{g}$ ) and micropore volume (microV,  $\text{cm}^3/\text{g}$ ), compared with the corresponding matrix 1 and 2, respectively. In our interpretation, this was due to the loaded captopril, which occupies also the interstitial microporosity, in good conformity with SEM images (spherical aggregates) (Figure 3).

While the SEM images evidence the presence of captopril in analysed systems, the EDAX results stress the carbon content corresponding to captopril content (Figure 3).

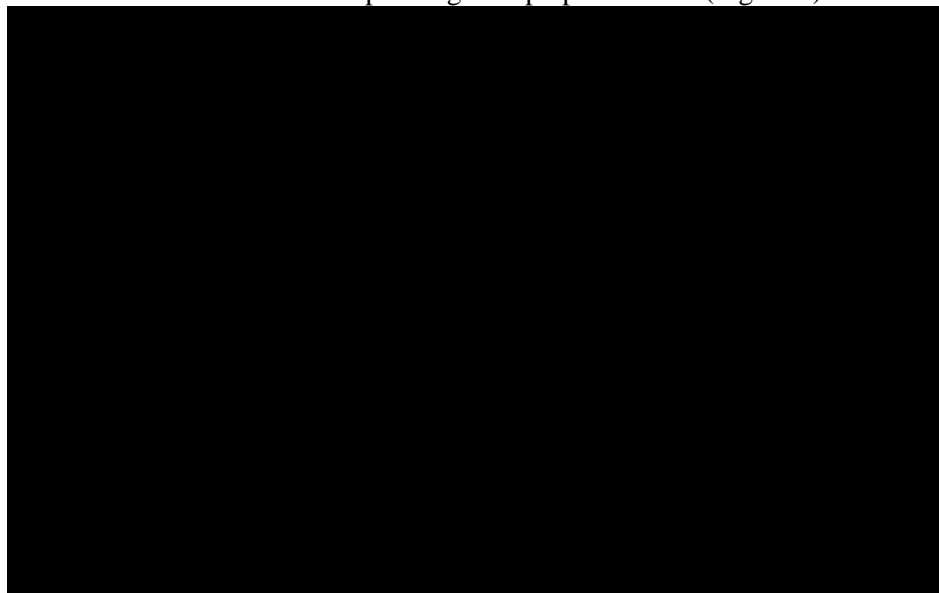


*Figure 4. The FTIR spectra of the system 2.*

The FTIR spectra (Figure 4) were performed to further demonstrate the presence of the drug in the matrix mesopores. After captopril loading, three characteristic absorption bands appear in the FTIR spectra. The quaternary carbon atom peak of the drug can be clearly observed at  $1450 \text{ cm}^{-1}$ . A weak shoulder appears at  $1702 \text{ cm}^{-1}$  and can be assigned to the C=O stretching of the drug. Additionally, the absorption band at  $1630 \text{ cm}^{-1}$  is shifted to lower wave number ( $1595 \text{ cm}^{-1}$ ). This shift can be attributed to the C=O stretching of amide in captopril. The weak shoulder at  $2877 \text{ cm}^{-1}$

is due to the symmetric CH<sub>3</sub> stretching mode of captopril. These observations confirmed that captopril was successfully loaded onto the mesoporous silica material.

### 3.2 Metabolic Parameters

#### a) Glucidic metabolism

The impact on glucidic metabolism was expressed by quantitative values of the following biochemical parameters: glycogen, glucose and lactic acid. As seen in Table 2 the *in vitro* treatment with captopril loaded on either functionalised or non functionalised silica matrix showed a significant decrease in glycogen and lactic acid content compared to cultures treated with captopril alone (group B - 100% captopril). It was also noticed a substantial difference in impact on these parameters between the cultures submitted to functionalized compared to non-functionalized substrate. Compared to group B (captopril free sample) the measured levels of glycogen, glucose and lactic acid in cultured treated with captopril loaded on APTES functionalized SBA-15 (group E) significantly decreased by 11,21%, 13% and 8%, respectively. No variation was noticed for the group C (cultures treated with SBA-15 alone) compared to control on any of the glucidic parameters studied.

Table 2. Glycogen, glucose and lactic acid concentrations (mg/g cellular mass)

	<b>Group A</b> control	<b>Group B</b> 100% captopril	<b>Group C</b> 0 % captopril	<b>Group D</b> 22.59% captopril	<b>Group E</b> 26.01% captopril
<b>Glycogen</b>	<b>30.15 ± 1.50</b> (5)	<b>17.39 ±1.25</b> (5)	<b>28.28 ±1.70</b> (5)	<b>22.18 ±1.34</b> (5)	<b>15.44 ±1.56</b> (5)
<i>p</i> value vs. A	-	<0.001	n.s.	<0.01	<0.001
<i>p</i> value vs. B	-	-	-	<0.05	n.s.
<i>p</i> value E vs D	-	-	-	-	<0.02
<b>Glucose</b>	<b>4.42 ±0.21</b> (5)	<b>3.37 ± 0.14</b> (5)	<b>4.13 ±0.25</b> (5)	<b>3.69 ± 0.19</b> (5)	<b>2.93 ±0.11</b> (5)
<i>p</i> value vs. A	-	<0.001	n.s.	<0.05	<0.001
<i>p</i> value vs. B	-	-	-	n.s.	<0.05
<i>p</i> value E vs D	-	-	-	-	<0.02
<b>Lactic acid</b>	<b>1.51±0.051</b> (5)	<b>1.25 ±0.013</b> (5)	<b>1.55±0.040</b> (5)	<b>1.34 ±0.016</b> (5)	<b>1.15±0.015</b> (5)
<i>p</i> value vs. A	-	<0.002	n.s.	<0.01	<0.001
<i>p</i> value vs. B	-	-	-	<0.01	<0.001
<i>p</i> value E vs D	-	-	-	-	<0.001

(Figures in brackets indicate the number of experimental cultures for each type).

### b) Lipidic Metabolism

The pattern of unfolding of the biochemical processes in the monkey kidney *Vero cells*, treated with free or carriers associated captopril was evaluated by the variation of the following 2 parameters: total lipids and free fatty acids.

Similar results were observed between groups A and C, showing no impact on lipidic metabolism of SBA-15.

Table 3. Total lipids and free fatty acids concentrations (mg/g cellular mass)

	<b>Group A</b> control	<b>Group B</b> 100% captopril	<b>Group C</b> 0 % captopril	<b>Group D</b> 22.59% captopril	<b>Group E</b> 26.01% captopril
<b>Total lipids</b>	<b>19.32± .05(5)</b>	<b>14.90±1.45 (5)</b>	<b>19.20 ± 1.55 (5)</b>	<b>15.85±1.12(5)</b>	<b>12.71±1.30(5)</b>
<i>p</i> value vs. A	-	<0.05	n.s.	<0.05	<0.01
<i>p</i> value vs. B	-	-	-	n.s.	n.s.
<i>p</i> value E vs D	-	-	-	-	n.s.
<b>Free fatty acids</b>	<b>5.55 ±0.25(5)</b>	<b>3.35 ±0.50(5)</b>	<b>5.42 ±0.37(5)</b>	<b>4.19±0.23(5)</b>	<b>2.07±0.30(5)</b>
<i>p</i> value vs. A	-	<0.01	n.s.	<0.01	<0.001
<i>p</i> value vs. B	-	-	-	n.s.	n.s.
<i>p</i> value E vs D	-	-	-	-	<0.001

(Figures in brackets indicate the number of experimental cultures for each type).

### c) Protidic Metabolism

Table 4. Total, soluble and insoluble proteins.

	<b>Group A</b> control	<b>Group B</b> 100% captopril	<b>Group C</b> 0 % captopril	<b>Group D</b> 22.59% captopril	<b>Group E</b> 26.01% captopril
<b>Total proteins</b>	<b>114.30±3.5(5)</b>	<b>101.42±3.8(5)</b>	<b>112.40±35(5)</b>	<b>105.43±4.0(5)</b>	<b>95.43±4.3(5)</b>
<i>p</i> value vs. A	-	<0.05	n.s.	<0.05	<0.01
<i>p</i> value vs. B	-	-	-	n.s.	n.s.
<i>p</i> value E vs D	-	-	-	-	n.s.
<b>Soluble proteins</b>	<b>76.20±1.7 (5)</b>	<b>63.40±2.0 (5)</b>	<b>74.26± 1.5(5)</b>	<b>67.34± 1.8(5)</b>	<b>56.42±2.0 (5)</b>
<i>p</i> value vs. A	-	<0.01	n.s.	<0.01	<0.001
<i>p</i> value vs. B	-	-	-	n.s.	<0.05
<i>p</i> value E vs D	-	-	-	-	<0.01

<b>Insoluble proteins</b>	<b>38.10±0.95(5)</b>	<b>38.02±1.35(5)</b>	<b>38.14±1.02(5)</b>	<b>38.09±1.24(5)</b>	<b>38.01±1.05(5)</b>
<i>p</i> value vs. A	-	n.s.	n.s.	n.s.	n.s.
<i>p</i> value vs. B	-	-	-	n.s.	n.s.
<i>p</i> value E vs D	-	-	-	-	n.s.

No statistical difference was also observed between groups B and D and B and E, respectively. Decreased fatty free acids concentration was observed in the group treated with captopril loaded on functionalised silica matrix (group E), compared to those treated with captopril loaded on non-functionalized matrix (group D), however, without an impact on the total amount of lipids.

Overall the samples did not show significant variation in total content of proteins. Among the drug containing samples, a significant decrease in soluble proteins was observed for samples treated with captopril on functionalised silica matrix compared to samples treated with either captopril free or captopril loaded on non-functionalized matrix. As noticed for the other metabolic parameters, no statistically significant differences were observed between groups C and A.

#### d) Nucleic acids

Although the total nucleic acid content did not vary in general among the groups, a variation was registered for between the groups treated with captopril loaded on functionalised versus non functionalized silica matrix (Table 5). This variation was mainly due to the influence on the RNA content. Again, SBA -15 treated group behaved similar to control group in terms of nucleic acids content.

Table 5. Deoxyribonucleic, ribonucleic and total nucleic acids concentrations (mg/g cellular mass) (Figures in brackets indicate the number of experimental cultures for each type).

	<b>Group A</b> control	<b>Group B</b>	<b>Group C</b>	<b>Group D</b> 22.59% captopril	<b>Group E</b> 26.01% captopril
<b>Total nucleic acids</b>	<b>148.7±4.0 (5)</b>	<b>115.9±4.5 (5)</b>	<b>147.7±4.0 (5)</b>	<b>127.8±3.3 (5)</b>	<b>107.1±3.8 (5)</b>
<i>p</i> value vs. A	-	<0.01	n.s.	<0.01	<0.001
<i>p</i> value vs. B	-	-	-	n.s.	n.s.
<i>p</i> value E vs D	-	-	-	-	<0.01
<b>Ribonucleic acid (RNA)</b>	116.5±3.0(5)	90.5 ±4.5 (5)	115.5 ±2.9 (5)	101.3±3.5 (5)	83.6 ± 3.9 (5)
<i>p</i> value vs. A	-	<0.002	n.s.	<0.02	<0.001
<i>p</i> value vs. B	-	-	-	n.s.	n.s.
<i>p</i> value E vs D	-	-	-	-	<0.01
<b>Desoxyribonucleic acid (DNA)</b>	32.2±1.7 (5)	25.4 ±1.4 (5)	32.2 ±1.5 (5)	26.5 ±1.3 (5)	23.5 ±2.00 (5)
<i>p</i> value vs. A	-	<0.02	n.s.	<0.05	<0.02
<i>p</i> value vs. B	-	-	-	n.s.	n.s.
<i>p</i> value E vs D	-	-	-	-	n.s.

#### 4. Discussion

Mesoporous silica nanoparticles are already used in various fields and more and more attention is given to their use in biomedical applications. Due to the small particle size, MSNs could act at cellular level, both at the extracellular space or within the cell [35]. In the light of this increased interest for their potential application in medical field, their behavior during interaction with normal cells should be addressed. The question of toxicity, as well as biocompatibility and metabolic impact, should be given an answer before any evaluation in humans is considered.

In 2008 di Pasqua reported the results of cytotoxicity of some mesoporous silica nanoparticles with BET surface areas varying from 825 to 200 m<sup>2</sup>/g, referring to the number of particles required to reduce normal cell growth by 50%. The author concluded that the most toxic mesoporous silica materials are those with the largest BET surface areas. Size and shape of the particles and the biocompatibility of the groups used for functionalization should be also taken into consideration. Hudson et al. reported the impact of mesoporous silica materials with particle size of 150 nm, 800 nm and 4 μm and pore size of 3nm, 7nm and 16 nm, respectively, on *in vitro* assays using human mesothelial cells, mouse peritoneal macrophage cells and mouse myoblast cells. The authors concluded that the toxicity of MCM-41, SBA-15 and MCF to mesothelial cells and myoblasts increased with the concentration of the particles (1,1, 3,3 and 5,5 mg/ml) most significantly on the mesothelial line [17].

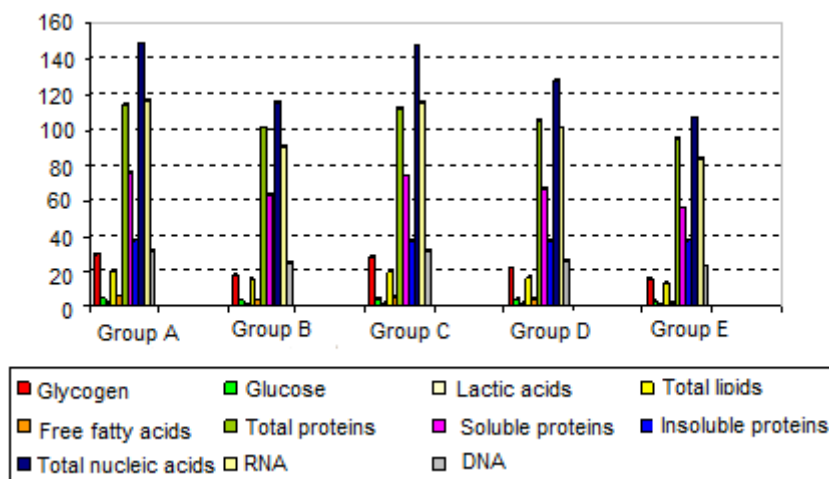


Fig. 5. Overall results of analysed metabolic parameters in the experimental groups.

In our research, we investigated the metabolic parameters in cells treated with an active substance loaded on various silica mesoporous drug delivery systems. Cytotoxicity of the mesoporous silica nanoparticles was evaluated mainly as impact on oxidative stress and normal cell growth. Although many reports were published regarding this topic, the effect on metabolic parameters was not yet investigated.

Our results on the *Vero cell* cultured treated with SBA -15 (BET surface area 862 m<sup>2</sup>/g) showed consistently no difference in evaluated parameters compared to control group (SBA-15 alone) in all three types of metabolism investigated. While a definite conclusion on cytotoxicity cannot be drawn based on only one observation, we acknowledge that at least at the doses used in our research (0.4 μg/flask) there is no indication of metabolic perturbances induced by SBA-15.

The outcome of the evaluation of glucidic metabolism showed an increase in oxygen consumption, which was greatest in the cultures treated with drug on functionalized mesoporous silica matrix, while in the samples treated with drug on non-functionalized matrix a limited activation of glucidic metabolism (mainly glycogenolysis and lactic acid consumption) was observed compared to captopril free treated samples.

The registered variations of the lipidic parameters have emphasized the intensification of the intracellular lipolysis and metabolic utilization of the free fatty acids by the different formulations of *in vitro* treatment with captopril.

Incubation of monkey renal *Vero cells* in the presence of associated captopril was correlated with protein reserves lower than that ones of the captopril-treated cultures. This finding was explained by an inhibitory impact induced by captopril on the biosynthesis of cell soluble proteins [38].

The experimental results have highlighted significant smaller amounts of RNA in drug on silica matrix in comparison to the captopril treated *Vero cultures*. Also, the perturbation of the biosynthesis of nucleic acids reconfirms the *in vitro* effect of captopril to induce the apoptotic phenomena on human vascular myocytes [36].

Interestingly, the metabolic effects observed with captopril on silica mesoporous matrix were greater than those with free captopril, while the quantity of captopril in the matrix 2 sample was approximately 4 times less than the captopril free. This potential dose sparing of the active substance carried on the functionalized drug delivery system was noticed only for functionalization with APTES, with less drug used, but stronger metabolic impact. An explanation for the overall findings might be related to the structural and functional differences of the two formulations used for the captopril transport, from which the bioactive agent is progressively released in the medium.

## 5. Conclusions

The impact on cellular parameters of captopril loaded on functionalized mesoporous silica-matrices was more accentuated than that of the free, unassociated drug. The optimized formulations modulate the metabolic processes in the monkey kidney *Vero cells* by the enhancing the glycogenolysis, glycolysis, and lipolysis and acting through an inhibitory effect upon protein and nucleic acids biosynthesis

The functionalized SBA-15/APTES mesoporous silica matrix could be an interesting direction for development of the new drug formulations.

Further investigation is needed to see if this observation applies also to the pharmacological effects, as it opens the possibility of obtaining a substantially increased effect of drugs at a much lower concentration and, therefore, less chances of related adverse events.

## References

- [1] I. Izquierdo-Barba, A. Martinez, A. L. Doadrio, J. Pérez-Pariente, M. Vallet-Regí, *Eur. J. Pharm. Sci.* **26**(5), 365 (2005).
- [2] M. Manzano, V. Aina, C. Arean, F. Balas, V. Cauda, M. Colilla, *Chem. Eng. J.* **137**(1), 30 (2008).
- [3] T. Heikkilä, J. Salonen, J. Tuura, M. S. Hamdy, G. Mul, N. Kumar, T. Salmi, D. Y. Murzin, L. Laitinen, A. M. Kaukonen, J. Hirvonen, V. Lehto, *Int. J. Pharm.* **331**(1), 133 (2007).
- [4] M. Vallet-Regí, F. Balas, D. Arcos, *Angew. Chem. Int. Ed. Engl.* **46**(40), 7548 (2007).
- [5] T. Linnell, J. Riikonen, J. Salonen, A. M. Kaukonen, L. Laitinen, J. Hirvonen, V. Lehto, *Int. J. Pharm.* **343**(1-2), 141 (2007).
- [6] B. G. Trewyn, J. A. Nieweg, Y. Zhao, V. S. Lin, *Chem. Eng. J.* **137**(1), 23 (2008).
- [7] A. L. Doadrio, E. M. B. Sousa, J. C. Doadrio, J. Pariente, I. Izquierdo-Barba, M. Vallet-Regí, *Control. Rel.*, **97**(1), 125 (2004).
- [8] I. Slowing, J. L. Vivero-Escoto, C. Wu, V. S. Lin, *Adv. Drug Deliv. Rev.* **60**(11), 1278 (2008).
- [9] S. Wang, *Micropor. Mesopor. Mater.* **121**, 73 (2009).
- [10] M. Vallet-Regí, *J. Intern. Med.* **267**(1), 22 (2010).
- [11] M. Veerapandian, K. Yun, *Digest J. Nanomater. Biostructures*, **4** (2), 243 (2009).
- [12] X. Huang, X. Teng, D. Chen, F. Tang, J. He, *Biomaterials* **31**, 438 (2010).
- [13] S. R. Bhattarai, E. Muthuswamy, A. Wani, M. Brichacek, A. L. Castañeda, S. Brock, D. Oupicky, *Pharm. Res.* **27**, 2556 (2010).
- [14] T. Ukmar, O. Planinsek, *Acta Pharm.* **60**, 373 (2010).
- [15] B. G. Trewyn, J. A. Nieweg, Y. Zhao, S. Victor, Y. Lin, *Chem. Engin. J.* **137**, 23 (2008).

- [16] A. Di Pasqua, K. K. Sharma, Y. L. Shi, B. B. Toms, W. Oullette, J. C. Dabrowiak, T. Asefa, *J. Inorg. Biochem.* **102**(7), 1416 (2008).
- [17] S. Hudson, R. F. Padera, R. Langer, D. S. Kohane, *Biomaterials*, **29**(30), 4045 (2008).
- [18] F. Wang, *Toxicology in Vitro*, **23**, 808 (2009).
- [19] Z. Tao, B. B. Toms, J. Goodisman, T. Asefa, *Chem. Res. Toxicol.* **22**(11), 1869 (2009).
- [20] A. Oscar, O. Carretero, *Am. J. Physiol. Heart Circ. Physiol.* **289**, 796 (2005).
- [21] P. C. Wu, Y. B. Huang, H. H. Lin, Y. H. Tsai, *Int. J. Pharm.* **103**(1), 119 (1996).
- [22] R.F. Popovici, E.M. Seftel, G.D. Mihai, E. Popovici, V.A. Voicu, *J Pharm Sci.* 2011 Feb; **100**(2):704-14.
- [23] D. Zhao, J. Feng, Q. Huo, N. Melosh, G. H. Fredrickson, B. F. Chmelka, *Science* **279**, 548 (1998).
- [24] D. Brühwiler, *Nanoscale* **2**, 887 (2010).
- [25] P. D. Tzanavaras, *The Open Chemical and Biomedical Methods Journal* **3**, 37(2010).
- [26] A. Doyle, J. B. Griffiths JB, *Cell and tissue culture: laboratory procedures in biotechnology*, John Wiley & Sons Ltd, West Sussex, (1998).
- [27] J. Scharfstein, V. Schmitz, V. Morandi, M. M. A. Capella, A. Lima, A. Morrot, L. Juliano, W. M.-Esterl, *J. Exp. Med* **192**(9), 1289 (2000).
- [28] P. L. Gardner, G. N. Mbuy, M. T. Knabb, *Life Sci.* **55**, (4), 283 (1994).
- [29] J. S. Coelho dos Santos, C. A. S. Menezes, F. N. A. Villani, L.M.D. Magalhães, J. Scharfstein, K. J. Gollob, W. O. Dutra, *Clinical Experimental Immunology* **162**, (3) 528 (2010).
- [30] A. Doyle, J. B. Griffiths, *Cell and tissue culture: laboratory procedures in biotechnology*, John Wiley & Sons Ltd, West Sussex, (1998).
- [31] Y. Yang, M. Xiao, Y. Mao, H. Li, S. Zhao, Y. Gu, R. Wang, J. Yu, X. Zhang, D. M. Irwin, G. Niu, H. Tan, *Biomed. Pharmacother.* **63**(5), 366 (2009).
- [32] L. Terri, Daines and Karen W. Morse, *J. Chem. Educ.* **53** (2), 126 (1976).
- [33] W. T. Hron, L. A. Menahan, *J. Lipid Res.* **22**(2), 377 (1981).
- [34] V. Artenie, E. Ungureanu, A. M. Negură, *Metode de investigare a metabolismului glucidic si lipidic*, Ed. PIM Iasi (2008).
- [35] J. M. Dawson, P. L. Heatlie, *Anal. Biochem.* **140** (2), 391 (1984).
- [36] M. B. Buemi, A. Allegra, D. Marino, M. T. Marino, M. A. Medici, G. De Pasquale, A. Ruello, F. Corica, N. Frisina, *Nephron.* **81**, 99 (1999).
- [37] D. Thassu, Y. Pathak, M. Deleers, *Nanoparticulate Drug-Delivery Systems: An Overview*, in *Drugs and the Pharmaceutical Sciences*, Editors D. Thassu, Y. Pathak, M. Deleers, Vol. 166 (2007).
- [38] O. V. Volpert, W. F. Ward, M. W. Lingen, L. Chesler, N. P. Bouck, *J. Clin. Invest.* **98** (3), 671 (1996).